Inelastic neutron scattering study of magnetic interactions in $CsMn_xMg_{1-x}Br_3$. II. Magnetic excitations in clusters of Mn^{2+} ions

U. Falk and A. Furrer
Labor für Neutronenstreuung, Eidgenössische Technische Hochschule Zürich, CH-5303 Würenlingen, Switzerland

N. Furer and H. U. Güdel
Institut für Anorganische Chemie, Universität Bern, CH-3000 Bern, Switzerland

J. K. Kjems
Risø National Laboratory, DK-4000 Roskilde, Denmark

(Received 10 October 1986)

Crystals of $CsMn_xMg_{1-x}Br_3$ with $x=0.14$, 0.28, 0.50, and 0.75 were synthesized and studied by inelastic neutron scattering (INS). Excitations of isolated Mn^{2+} dimers, trimers, and tetramers could be identified on the basis of their characteristic dependences on temperature and momentum transfer. They show no energy dispersion and can be observed in all the crystals studied. From the observed energy splittings the following exchange parameters were deduced: $J_{\text{dimer}}=-838$ μeV (bilinear exchange), $K_{\text{dimer}}=8.8$ μeV (biquadratic exchange); $J_{\text{trimer}}=-777$ μeV, $J'_{\text{trimer}}=-11$ μeV (second-nearest-neighbor bilinear exchange), $K_{\text{trimer}}=8.4$ μeV, $L=6.1$ μeV (three-center interaction). Second-nearest-neighbor exchange as well as two- and three-center biquadratic terms significantly contribute to the exchange coupling. The bulk properties of pure $CsMnBr_3$ can be reproduced with the parameters derived for the small clusters. INS spectra of the $x=0.50$ and $x=0.75$ crystals show two distinctly different types of excitations: relatively sharp bands with no energy dispersion which are predominantly due to dimer and trimer transitions; superimposed is a broad band, more intense in the $x=0.75$ spectrum, with spin-wave-like energy dispersion. The applicability and limits of cluster and spin-wave models to account for the observed INS features are discussed.

I. INTRODUCTION

In a previous paper (paper I, Ref. 1) we demonstrated that the spin-wave dispersion of the one-dimensional (1D) Heisenberg antiferromagnet $CsMnBr_3$ can be well accounted for by an effective Hamiltonian of the form

$$\mathcal{H}=-2\sum_{i>j}J_{ij}\mathbf{S}_i\cdot\mathbf{S}_j+D\sum_i(S_i^z)^2 \tag{1}$$

in which the sum $\sum_{i>j}$ includes all the nearest neighbors within and between the chains of Mn^{2+} ions, and the J_{ij}'s are phenomenological exchange parameters. In the present paper we wish to explore the applicability of the Heisenberg model and the various contributions to the J_{ij}'s in some more detail by studying small clusters of exchange coupled Mn^{2+} ions in mixed crystals of composition $CsMn_xMg_{1-x}Br_3$ ($x=0.14$, 0.28, 0.50, 0.75). We also want to address the question whether a cluster model which was successfully applied to interpret the neutron spectroscopic data for Mn^{2+} concentrations $x\leq 0.28$, or a spin-wave model is more adequate for a description of the magnetic excitations for $x\geq 0.50$.

In contrast to magnetic systems with extended interactions small clusters of magnetic ions have the advantage that the relevant exchange Hamiltonian can be solved exactly. The magnetic excitations have localized molecular character and thus show no energy dispersion. As a result the cluster energy levels can be experimentally determined with great accuracy. We chose mixed crystals of $CsMnBr_3$ and $CsMgBr_3$ for various reasons. Both compounds crystallize in the hexagonal space group $P6_3/mmc$, and their unit cells are the same within experimental accuracy: $a=7.61$ Å, $c=6.50$ Å.[2] The structure consists of chains of face-sharing MBr_6 ($M=Mn^{2+}$, Mg^{2+}) octahedra parallel to the c axis. $CsMnBr_3$ exhibits pronounced 1D magnetic behavior with J'' (interchain) approximately 3 orders of magnitude smaller than J (intrachain).[1] As a result J'' can in good approximation be neglected in the study of clusters in the mixed crystals. All the clusters are thus linear chain fragments with composition Mn_nBr_{3n+1} oriented parallel to the c axis. In contrast to three-dimensional (3D) systems, in which the number of structural isomers increases very strongly with increasing cluster size and thus complicates the situation, there are no isomers in our 1D system. Mixed crystals $CsMn_xMg_{1-x}Br_3$ can be synthesized for any value of x. The concentration x is therefore an important experimental variable, which determines the cluster size distribution. Since the unit cells of the two constituents are the same, it is a good assumption that the distribution of Mn^{2+} and Mg^{2+} ions is statistical.

The Mn^{2+} ion is a very close realization of a spin-only magnetic center. Its free-ion ground state is ^6S, and in the (slightly trigonally distorted) octahedral crystal field it is $^6A_{1g}$ with $g=2.00$.[3] It is thus an ideal candidate for Heisenberg interactions with $S=\frac{5}{2}$.

The technique used in this study to explore the magnetic cluster excitations is inelastic neutron scattering (INS).

It allows a discrimination between magnetic and phonon excitations on the basis of their dependence on temperature T and scattering vector $\mathbf{Q}$. It offers an additional advantage over optical spectroscopic techniques (IR, Raman spectroscopy) in the study of magnetic excitations. This is based on the fact that neutrons, in contrast to photons, can directly interact with the spin system. As a consequence, excitations within the exchange-split ground manifold are observable, while they are forbidden for photon spectroscopy. As we show in Sec. II, excitation intensities of the various clusters (dimers, trimers, etc.) all have different $\mathbf{Q}$ dependences. They can thus experimentally be distinguished. An important and fundamental question for understanding magnetic interactions is concerned with higher-order exchange terms in the Hamiltonian. How relevant are effects like biquadratic exchange and three-center interactions? We will demonstrate that the study of dimers and trimers in $CsMn_xMg_{1-x}Br_3$ provides quantitative answers to this question.

II. THEORY

A. Energy splittings

The Heisenberg model is based on the bilinear spin permutation operator

$$P_{ij}=\tfrac{1}{2}(1+\mathbf{S}_i\cdot\mathbf{S}_j)\ . \tag{2}$$

A more complete Hamiltonian takes permutations of more than two spins into account. The relevant terms up to second order (biquadratic terms) can be written as

$$P_{ij}^2=\tfrac{1}{4}[1+2\mathbf{S}_i\cdot\mathbf{S}_j+(\mathbf{S}_i\cdot\mathbf{S}_j)^2]\ , \tag{3a}$$

$$P_{ij}P_{jk}=\tfrac{1}{4}[1+\mathbf{S}_i\cdot\mathbf{S}_j+\mathbf{S}_j\cdot\mathbf{S}_k+(\mathbf{S}_i\cdot\mathbf{S}_j)(\mathbf{S}_j\cdot\mathbf{S}_k)]\ , \tag{3b}$$

$$P_{ij}P_{kl}=\tfrac{1}{4}[1+\mathbf{S}_i\cdot\mathbf{S}_j+\mathbf{S}_k\cdot\mathbf{S}_l+(\mathbf{S}_i\cdot\mathbf{S}_j)(\mathbf{S}_k\cdot\mathbf{S}_l)]\ . \tag{3c}$$

The expressions (3a), (3b), and (3c) refer to two-spin, three-spin, and four-spin interactions, respectively. All these interactions are isotropic. Anisotropy effects may arise from the single-ion anisotropy and magnetic dipole-dipole coupling. Zero-field splittings of Mn^{2+} ions in a similar ligand environment have been found by EPR to be of the order of 0.02 meV.[3] Magnetic dipole-dipole interactions have an isotropic part which is included in the parameter J. The anisotropic part is calculated to be smaller than 0.02 meV. In comparison with the exchange energies, these anisotropy energies are considered to be negligible.

For a dimer the exchange Hamiltonian, up to second order in spin operators, can be written as

$$\mathcal{H}_{\text{dimer}}=-2J\mathbf{S}_1\cdot\mathbf{S}_2-K(\mathbf{S}_1\cdot\mathbf{S}_2)^2\ , \tag{4}$$

where J and K are bilinear and biquadratic exchange parameters, respectively. Equation (4) is diagonal in the basis $|S,M\rangle$ where S denotes the total dimer spin $\mathbf{S}=\mathbf{S}_1+\mathbf{S}_2$. For $S_1=S_2=\frac{5}{2}$ the total spin can take any integer value between 0 and 5, and the eigenvalues are given by

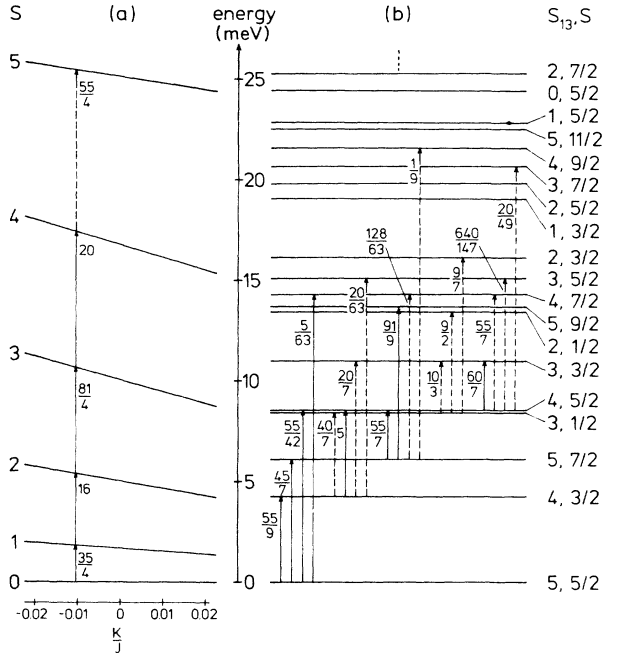

FIG. 1. (a) Calculated Mn^{2+} dimer energy levels using Eq. (5). Allowed INS transitions are indicated with the square of their transition matrix elements. Solid and dashed arrows denote observed and unobserved transitions, respectively. The energy scale corresponds to $J=-838$ μeV. (b) Low-energy part of Mn^{2+} trimer exchange splitting pattern, calculated with Eq. (7) and the parameters given in Sec. V B. Transitions are indicated as in (a).

$$E(S)=(-J+\tfrac{35}{4}K)S(S+1)-\tfrac{1}{4}KS^2(S+1)^2+\tfrac{35}{2}(J-\tfrac{35}{8}K)\ . \tag{5}$$

The energy splitting pattern is shown in Fig. 1(a) for antiferromagnetic exchange as a function of the ratio K/J.

For a linear trimer the exchange Hamiltonian is given by

$$\mathcal{H}_{\text{trimer}}=-2J(\mathbf{S}_1\cdot\mathbf{S}_2+\mathbf{S}_2\cdot\mathbf{S}_3)-2J'\mathbf{S}_1\cdot\mathbf{S}_3-K[(\mathbf{S}_1\cdot\mathbf{S}_2)^2+(\mathbf{S}_2\cdot\mathbf{S}_3)^2]-K'(\mathbf{S}_1\cdot\mathbf{S}_3)^2-L[(\mathbf{S}_1\cdot\mathbf{S}_2)(\mathbf{S}_2\cdot\mathbf{S}_3)+(\mathbf{S}_3\cdot\mathbf{S}_2)(\mathbf{S}_2\cdot\mathbf{S}_1)]\ , \tag{6}$$

where J' and K' are second-nearest-neighbor exchange parameters and L represents three-center interactions. We use the coupling scheme: $\mathbf{S}_{13}=\mathbf{S}_1+\mathbf{S}_3$ and $\mathbf{S}=\mathbf{S}_{13}+\mathbf{S}_2$. With $0\le S_{13}\le 5$ and $|S_{13}-\frac{5}{2}|\le S\le S_{13}+\frac{5}{2}$ we obtain a total of 27 spin levels. For dominant bilinear interactions Eq. (6) can be solved to a good approximation by first-order perturbation theory in the basis $|S_{13},S\rangle$. The energies are then

$$E(S_{13},S)=-JS(S+1)+(J-J'+\tfrac{35}{4}K')S_{13}(S_{13}+1)-\tfrac{1}{4}K'S_{13}^2(S_{13}+1)^2-K\langle S_{13},S\,|\,(\mathbf{S}_1\cdot\mathbf{S}_2)^2+(\mathbf{S}_2\cdot\mathbf{S}_3)^2\,|\,S_{13},S\rangle-L\langle S_{13},S\,|\,(\mathbf{S}_1\cdot\mathbf{S}_2)(\mathbf{S}_2\cdot\mathbf{S}_3)+(\mathbf{S}_3\cdot\mathbf{S}_2)(\mathbf{S}_2\cdot\mathbf{S}_1)\,|\,S_{13},S\rangle+\tfrac{35}{4}(J+2J'-\tfrac{35}{4}K')\ . \tag{7}$$

The expectation values of the low-lying trimer levels were given in Ref. 4. The corresponding splitting pattern is shown in Fig. 1(b).

For clusters with four and more (n) Mn^{2+} centers there exists no simple basis of functions which diagonalizes the bilinear Heisenberg Hamiltonian

$$\mathcal{H}=-2J\sum_{i=1}^{n-1}\mathbf{S}_i\cdot\mathbf{S}_{i+1}\ . \tag{8}$$

The total spin S and M remain the only good quantum numbers. The full energy matrix has to be evaluated and diagonalized, which becomes progressively more cumbersome as n increases. For dominant antiferromagnetic nearest-neighbor exchange J the low-energy part of the splitting patterns for $n=4,5,6$ is given in Fig. 2. The ground level for antiferromagnetic clusters with an even number of Mn^{2+} centers is always a spin singlet as expected.

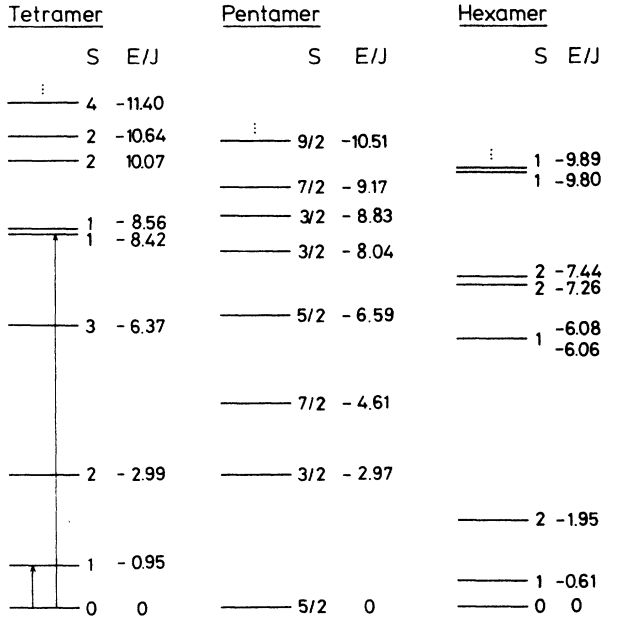

FIG. 2. Low-energy part of Mn^{2+} tetramer, pentamer, and hexamer exchange splitting pattern, calculated by diagonalizing the energy matrix of Eq. (8). The arrows denote the observed tetramer transitions.

B. Neutron cross section

The cross section for a transition $|\tau,S\rangle\rightarrow|\tau',S'\rangle$ in a system of isolated clusters of magnetic ions can be brought to the following form:[5]

$$\frac{d^2\sigma}{d\Omega\,d\omega}=C\exp\left[-\frac{E(S)}{k_BT}\right]\sum_{\alpha,\beta}\left[\delta_{\alpha\beta}-\frac{Q_\alpha Q_\beta}{Q^2}\right]\sum_{j,j'}\exp[i\mathbf{Q}\cdot(\mathbf{R}_j-\mathbf{R}_{j'})]\sum_{M,M'}\langle\tau SM\,|\,S_j^\alpha\,|\,\tau'S'M'\rangle\langle\tau'S'M'\,|\,S_{j'}^\beta\,|\,\tau SM\rangle$$
$$\times\delta[\hbar\omega+E(S)-E(S')] \tag{9}$$

and

$$C=\frac{N}{Z}\left[\frac{\gamma e^2}{m_ec^2}\right]^2\frac{k'}{k}F^2(\mathbf{Q})\exp[-2W(\mathbf{Q})]\ .$$

N is the total number of magnetic clusters in the sample, Z the partition function, k and k' the wave numbers of the incoming and scattered neutrons, respectively, $\mathbf{Q}=\mathbf{k}-\mathbf{k}'$ is the scattering vector, $F(\mathbf{Q})$ the magnetic form factor, $\exp[-2W(\mathbf{Q})]$ the Debye-Waller factor, and $\mathbf{R}_j$ the position vector of the jth magnetic ion in the cluster. $\alpha,\beta=x,y,z$. S denotes the total cluster spin and τ stands for other quantum numbers which characterize the cluster level. For dimers and trimers of identical spins the cross section for transitions $|S\rangle\rightarrow|S'\rangle$ and $|S_{13},S\rangle\rightarrow|S'_{13},S'\rangle$, respectively, simplifies to

$$\left[\frac{d^2\sigma}{d\Omega\,d\omega}\right]_{\text{dimer}}=C'p(S)F^2(\mathbf{Q})\,|\,T_{S\rightarrow S'}\,|^2$$
$$\times[1+(-1)^{S+S'}\cos(\mathbf{Q}\cdot\mathbf{R}_{12})]\ , \tag{10}$$

and

$$\left[\frac{d^2\sigma}{d\Omega\,d\omega}\right]_{\text{trimer}}=C''p(S_{13},S)F^2(\mathbf{Q})\,|\,T_{S_{13},S\rightarrow S'_{13},S'}\,|^2\{1+(-1)^{S_{13}+S'_{13}}\cos(\mathbf{Q}\cdot\mathbf{R}_{13})$$
$$+2\delta(S_{13},S'_{13})[1-\cos(\mathbf{Q}\cdot\mathbf{R}_{12})-\cos(\mathbf{Q}\cdot\mathbf{R}_{23})]\}\ . \tag{11}$$

All the constant factors which are irrelevant in the present context are summarized in the constants C' and C''. $p(S)$ and $p(S_{13},S)$ are Boltzmann population factors and $\mathbf{R}_{ij}=\mathbf{R}_i-\mathbf{R}_j$. $T_{S\to S'}$ and $T_{S_{13},S\to S'_{13},S'}$ are transition matrix elements defined in Ref. 5. The following selection rules are easily derived from the cross-section formulas:

$$\text{Dimer excitations: } \Delta S=0,\pm1\ ,\quad \Delta M=0,\pm1\ , \tag{12a}$$

$$\text{Trimer excitations: } \Delta S=0,\pm1\ ,\quad \Delta M=0,\pm1\ ,\quad \Delta S_{13}=0,\pm1\ . \tag{12b}$$

Allowed transitions are indicated by arrows and the square of the corresponding matrix element in Fig. 1.

The expressions in square brackets in Eqs. (10) and (11) are so-called interference terms.[6] They reflect the geometry of the cluster and its orientation in the crystal. Together with the form factor these interference terms determine the **Q** dependence of the cross section. Figure 3 shows the calculated **Q** dependence of the interference terms for dimer and trimer excitations. The modulations resulting from the interference term are seen to be characteristic for a given transition. Trimer excitations with $\Delta S_{13}=0$ and $\Delta S_{13}=\pm1$, e.g., have the opposite behavior between $\mathbf{Q}=(0,0,1.0)$ and $(0,0,1.5)$.

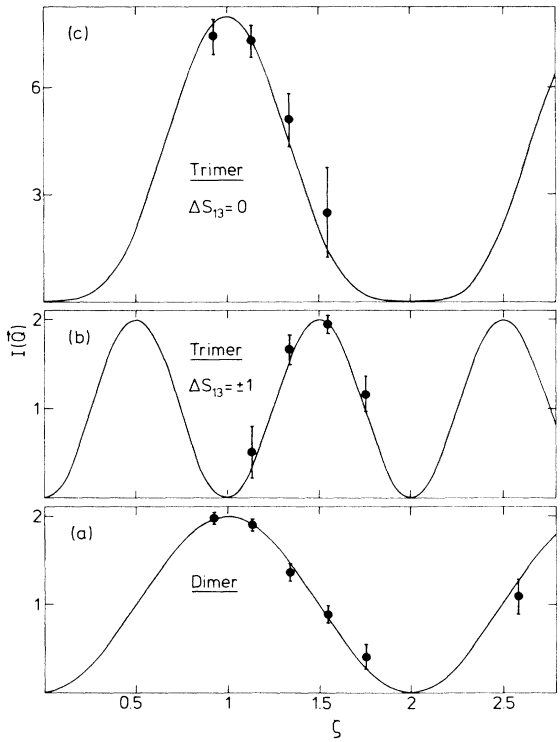

FIG. 3. Dimer and trimer excitation intensities observed for $CsMn_{0.28}Mg_{0.72}Br_3$ at $T=5$ K and $\mathbf{Q}=(0,0,\xi)$. The solid lines correspond to the interference terms of Eqs. (10) and (11). (a) Dimer transition $|0\rangle\to|1\rangle$; (b) trimer transition $|5,\frac{5}{2}\rangle\to|4,\frac{3}{2}\rangle$; (c) trimer transition $|5,\frac{5}{2}\rangle\to|5,\frac{7}{2}\rangle$.

III. EXPERIMENTAL

The following starting materials were used for the syntheses: CsBr (Merck, suprapur), $MnCO_3\cdot nH_2O$ (Merck, *pro analysi*), $MgBr_2$ (Ventron), HBr solution (Merck, suprapur, 47%), HBr gas (Merck, 99.8%). $CsMgBr_3$ was prepared by melting stoichiometric amounts of CsBr and $MgBr_2$ in a stream of dry HBr at 700 °C.

$CsMnBr_3$ was synthesized as follows: $MnCO_3\cdot nH_2O$ was dissolved in an excess of 10% aqueous HBr. One-fifth of the stoichiometric amount of CsBr was added and the solution was slowly evaporated at 50 °C. The first fraction of crystals consists of platelike $CsMnBr_3\cdot 2H_2O$. They were separated by filtration and then dehydrated at 130 °C in an oven. For a complete removal of H_2O the powder was placed in a large ampoule, which was slowly heated under vacuum ($<10^{-4}$ Torr) to 300 °C. For the synthesis of mixed crystals $CsMn_xMg_{1-x}Br_3$ the appropriate amounts of $CsMnBr_3$ and $CsMgBr_3$ were mixed and placed in graphitized silica ampoules of 7 mm inner diameter. This mixture was heated under vacuum to 300 °C until the pressure was smaller than 10^{-5} Torr. The ampoule was then sealed and placed in a Bridgman furnace for crystal growth. Pulling rates were between 0.01 and 0.03 mm/min. All the anhydrous materials are air sensitive, and consequently all the manipulations were done in the inert atmosphere of a dry box.

Single crystals of typically 15 mm length were oriented so as to place the (101) plane into the scattering plane. The majority of the INS experiments were performed at the reactor Saphir in Würenlingen with use of the triple-axis spectrometers R2 and R5. Either the incoming or outgoing energy of the neutrons was kept fixed at 13.7 or 15.0 meV. High-resolution INS experiments were performed at the DR3 reactor in Risø with use of the triple-axis spectrometer TAS7 which is installed at a neutron guide connected to a cold H_2 source. The scattered neutron energy was held constant at 5.0 meV, giving rise to an energy resolution of 0.28 meV. To gain intensity all experiments were carried out with use of a vertically or doubly bent graphite monochromator as well as a horizontally bent graphite analyzer, with the (002) planes as scattering planes for most scans. Pyrolitic graphite or cooled beryllium filters were inserted into the neutron beam to reduce higher-order contamination. The measurements were carried out in the neutron energy-loss configuration for several scattering vectors $\mathbf{Q}=(0,0,\zeta)$ in the temperature range $2\text{ K}\le T\le 70$ K.

IV. RESULTS

Figure 4 shows energy loss INS spectra of $CsMn_xMg_{1-x}Br_3$ crystals with composition $x=0.14$, 0.28, 0.50, and 0.75 at low temperatures. A band at 1.8 meV dominates the spectra up to $x=0.50$. Its position is independent of concentration and it is still discernible in the $x=0.75$ spectrum, where it is superimposed on a rather intense broad background. This 1.8 meV excitation is

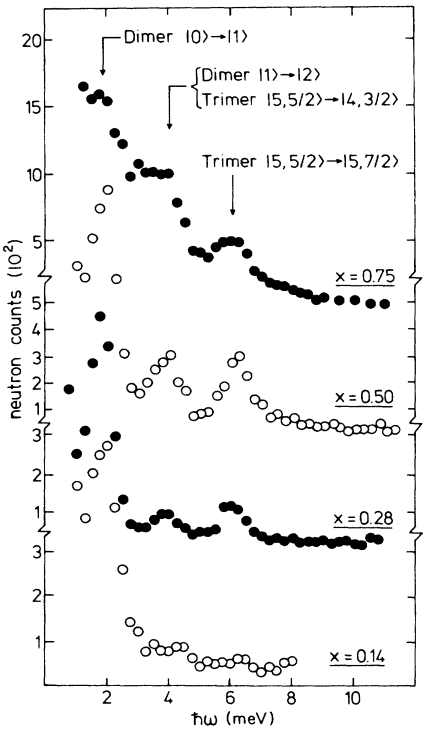

FIG. 4. Low-temperature INS spectra of $CsMg_{1-x}Mn_xBr_3$ for various values of x. $\mathbf{Q}=(0,0,1.1)$. $T=5$ K and 10 K for $x<0.50$ and $x\geq 0.50$, respectively.

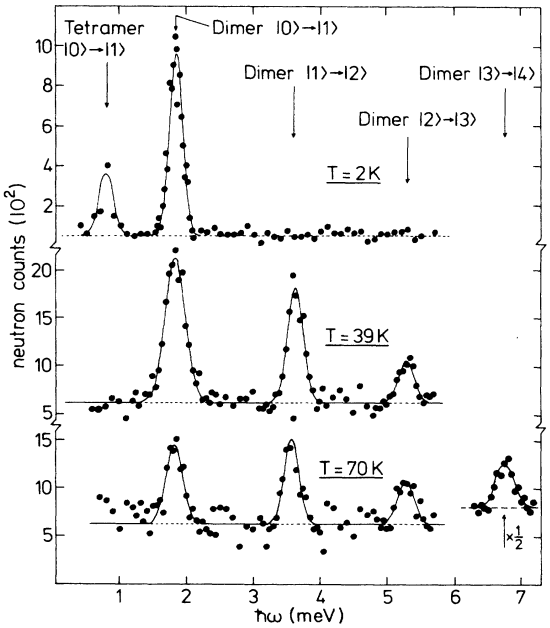

FIG. 5. Inelastic neutron scattering of $CsMn_{0.28}Mg_{0.72}Br_3$ for $\mathbf{Q}=(0,0,1.0)$ showing Mn^{2+} dimer and tetramer excitations as indicated. The dimer transition $|3\rangle\rightarrow|4\rangle$ was measured at $\mathbf{Q}=(0,0,1.4)$. The counting time for the energy spectrum taken at $T=2$ K was 6 times shorter than for the other spectra. The lines are the result of Gaussian least-squares fits to the observed data.

readily identified from its temperature and Q dependence (Fig. 3) as the $|0\rangle\rightarrow|1\rangle$ dimer transition. Two sharp bands at approximately 4 and 6 meV show up prominently in the $x=0.28$ and $x=0.50$ crystals. They are readily assigned to dimer and trimer excitations as indicated in Fig. 4.[7] Their Q dependences are included in Fig. 3. As predicted by the theory, they are distinctly different. In the $x=0.75$ spectrum these trimer excitations can still be identified, but they represent only a relatively small fraction of the total inelastic scattering. In the $x=0.28$ spectra of Fig. 5 $\mathbf{Q}=(0,0,1.0)$ was chosen to maximize the intensity of dimer excitations as well as to avoid $\Delta S_{13}=\pm 1$ trimer excitations. As a consequence four $\Delta S=1$ dimer transitions are observable. The temperature dependence of their intensities is governed by Boltzmann statistics. Their observed widths correspond to the instrumental resolution, i.e., we can detect no physical broadening and thus conclude that any anisotropy effects, which would lift the M degeneracy of the dimer levels, must be smaller than the observed line widths. The lowest energy band at 0.76 meV in the 2 K spectrum of Fig. 5 corresponds to the lowest energy $|S\rangle\rightarrow|S'\rangle=|0\rangle\rightarrow|1\rangle$ tetramer excitation. Another $|0\rangle\rightarrow|1\rangle$ excitation is observed at 7.03 meV as shown in Fig. 6, which also shows the 4.27 and 6.10 meV trimer transitions. For this experiment $\mathbf{Q}=(0,0,1.5)$ was chosen to maximize the intensity of trimer $\Delta S_{13}=\pm 1$ transitions and, at the same time, minimize the dimer excitations.

Figure 7 shows the results of INS experiments at 10 K on the most concentrated ($x=0.75$) crystal. The inelastic scattering is strongly Q dependent between $\mathbf{Q}=(0,0,1)$ and $(0,0,1.5)$. Two distinct types of behavior are observed. The three relatively sharp peaks at approximately 2, 4, and 6 meV show no energy dispersion. Their intensities, however, are Q dependent. The three transitions have already been assigned as localized dimer and trimer excitations. The bulk of the inelastic scattering in Fig. 7, on the other hand, shows energy dispersion. For ζ values close to one the main intensity is centered close to zero energy

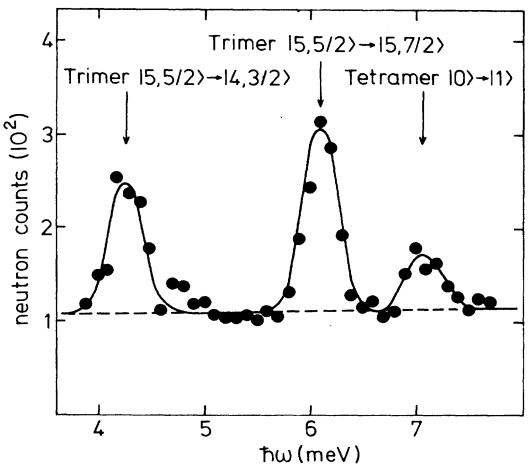

FIG. 6. INS spectrum of $CsMn_{0.28}Mg_{0.72}Br_3$ at $T=4.5$ K and $\mathbf{Q}=(0,0,1.5)$. The peaks are assigned as indicated. The lines are as in Fig. 5.

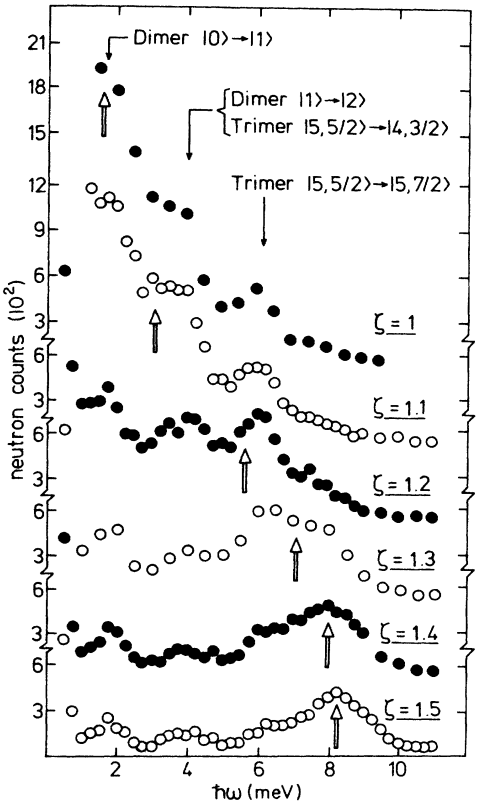

FIG. 7. $\mathbf{Q}=(0,0,\zeta)$ dependence of INS from $CsMn_{0.75}Mg_{0.25}Br_3$ observed at $T=10$ K. Three dimer and trimer excitations are indicated by single arrows. Spin-wave-like excitations are indicated by double arrows.

TABLE I. Observed and calculated energies of cluster excitations in $CsMn_{0.28}Mg_{0.72}Br_3$. The calculated energies for the dimer, trimer, and tetramer excitations result from Eqs. (5), (7), and (8), respectively, with the corresponding coupling parameters given in Sec. V. For the tetramer $J=-834$ μeV was used.

Cluster	Assignment	$\hbar\omega_{obs}$ (meV)	$\hbar\omega_{calc}$ (meV)
Dimer	$\|0\rangle\rightarrow\|1\rangle$	1.80±0.01	1.82
	$\|1\rangle\rightarrow\|2\rangle$	3.60±0.01	3.59
	$\|2\rangle\rightarrow\|3\rangle$	5.27±0.02	5.25
	$\|3\rangle\rightarrow\|4\rangle$	6.74±0.03	6.76
Trimer	$\|5,\frac{5}{2}\rangle\rightarrow\|4,\frac{3}{2}\rangle$	4.27±0.03	4.27
	$\|5,\frac{5}{2}\rangle\rightarrow\|5,\frac{7}{2}\rangle$	6.10±0.02	6.10
	$\|5,\frac{5}{2}\rangle\rightarrow\|4,\frac{5}{2}\rangle$	8.52±0.09	8.53
	$\|5,\frac{5}{2}\rangle\rightarrow\|4,\frac{7}{2}\rangle$	14.74±0.15	14.37
	$\|4,\frac{3}{2}\rangle\rightarrow\|4,\frac{5}{2}\rangle$	4.21±0.08	4.26
	$\|5,\frac{7}{2}\rangle\rightarrow\|4,\frac{5}{2}\rangle$	2.45±0.10	2.44
	$\|5,\frac{7}{2}\rangle\rightarrow\|5,\frac{9}{2}\rangle$	7.58±0.05	7.58
	$\|4,\frac{5}{2}\rangle\rightarrow\|3,\frac{3}{2}\rangle$	2.45±0.10	2.44
Tetramer	$\|0\rangle\rightarrow\|1\rangle$	0.76±0.04	0.79
	$\|0\rangle\rightarrow\|1\rangle$	7.03±0.05	7.02

transfer. As ζ varies from 1.0 to 1.5, a broad peak moves to higher energy and reaches a final position of approximately 8 meV at $\mathbf{Q}=(0,0,1.5)$. Its width appears to decrease with increasing ζ, and its position, indicated by a double arrow in Fig. 7, is better defined for large ζ. The behavior of this band is typical of a collective excitation, and it is reminiscent of the spin-wave excitations in pure $CsMnBr_3$.[1] The $x=0.50$ crystal shows a similar Q dependence. But in this case the dimer and trimer excitations still dominate the inelastic intensity.

Table I shows a comparison of observed and calculated dimer, trimer, and tetramer excitation energies. Within experimental error there is no difference of the observed exchange splittings for $x=0.14$ and $x=0.28$. For $x=0.50$ and $x=0.75$ no detailed data analysis was performed.

V. ANALYSIS AND DISCUSSION

A. Dimer excitations

The energies of the dimer excitations approximately follow the Landé interval rule expected for bilinear exchange only. As shown in Table I, the substantial deviations observed for the $|2\rangle\rightarrow|3\rangle$ and $|3\rangle\rightarrow|4\rangle$ transitions are accounted for by the inclusion of a biquadratic term in the Hamiltonian, i.e., by the use of Eq. (5). The parameter values obtained from a least-squares fit to the data are

$$J_{\text{dimer}}=-838\pm5\ \mu\text{eV}\ ,$$

$$K_{\text{dimer}}=8.8\pm0.8\ \mu\text{eV}\ .$$

The biquadratic parameter is of the order of 1% of the bilinear parameter, however, the corresponding corrections of the dimer energy levels can be up to 4% as shown in Fig. 1(a). We have demonstrated in a previous publication that exchange striction is a likely physical origin of the biquadratic term.[8] A value of

$$\left[\frac{\delta J}{\delta R}\right]^2_{R_0}\simeq200\ (\text{meV}/\text{Å})^2$$

was estimated, which typically corresponds to a 15% change of J when the Mn-Mn distance is compressed or expanded by 0.01 Å. The spin-wave dispersion of $CsMnBr_3$ can be excellently reproduced by the above dimer parameters. Similarly, the magnetic susceptibility is much better reproduced, particularly at temperatures below 100 K, by our parameters than by a model with only bilinear exchange.[9]

B. Trimer excitations

For the assignment of the eight observed trimer transitions their T and $\mathbf{Q}$ dependence was used in addition to their energies, which were approximately predictable on the basis of the dimer parameters.[4] For an evaluation of exchange parameters Eq. (7) was fitted to the observed transition energies by a least-squares procedure. The result obtained with the following set of parameters is shown in Table I:

$J=-777\pm6$ μeV ,

$J'=-11\pm9$ μeV ,

$K=8.4\pm0.9$ μeV ,

$L=6.1\pm0.6$ μeV ,

K' set to zero .

Fits were also made with L set to zero as well as K and L set to zero. They were significantly worse.[4] In particular, by the inclusion of L the standard deviation χ^2 of calculated and measured transition energies was reduced by a factor of 1.9. From this we conclude that three-center interaction terms significantly contribute to the exchange coupling. This is a result of fundamental importance. Despite numerous theoretical predictions direct experimental evidence for the existence of such interactions has been lacking so far. L is found to be of the same order of magnitude as K, the biquadratic two-center parameter. This is theoretically not unexpected since both terms appear in the same order of perturbation theory in the treatment of exchange interactions. Since K is likely due to exchange striction, it is of course tempting to attribute L to magnetostrictive forces as well. For $\tilde{K}=K=L$ and $K'=0$ Eq. (6) simplifies to

$$\mathcal{H}_{\text{trimer}}=-2J(\mathbf{S}_1\cdot\mathbf{S}_2+\mathbf{S}_2\cdot\mathbf{S}_3)-2J'\mathbf{S}_1\cdot\mathbf{S}_3 -\tilde{K}(\mathbf{S}_1\cdot\mathbf{S}_2+\mathbf{S}_2\cdot\mathbf{S}_3)^2 \quad (13)$$

with $\tilde{K}$ as an overall magnetostrictive parameter.

In conclusion, the large number of eight observed trimer transition energies leads to accurate exchange parameters and thus a very detailed picture of the various contributions to the exchange coupling. It is quite clear that this cannot be obtained from the spin-wave dispersion of the concentrated material $CsMnBr_3$, the information content of which is much smaller.

C. Tetramer excitations

The two peaks at 0.76 and 7.03 meV, which we assigned to tetramer $|0\rangle\rightarrow|1\rangle$ excitations, have different Q dependences. The low-energy transition has maximum intensity at Q=(0,0,1.0) and disappears at Q=(0,0,1.5), whereas the high-energy peak was measured at Q=(0,0,1.5). On the basis of Fig. 2 and the selection rule $\Delta S=0,\pm1$, the 0.76 meV peak is assigned to the $-0.95J$ excitation and the 7.03 meV peak either to the $-8.42J$ or the $-8.56J$ excitation or a superposition of both. A calculation of the INS cross section shows that only the $-8.42J$ transition has nonvanishing intensity at Q=(0,0,1.5), and the assignment can be made.

It is, of course, not possible to deduce a set of exchange parameters as we did for the trimers from only two observables. But it is interesting to investigate whether the two excitation energies can be reproduced by the parameters derived for the trimers. Using the parameters given in Sec. V B we obtain 0.78 and 7.35 meV for the two tetramer excitations. The 0.3 meV difference to the experimental value of the high-energy transition is significant. We conclude that the tetramer exchange parameters are slightly different from the trimer parameters. A similar observation was made when going from the dimers to the trimers. Furthermore, four-center interaction terms based on the permutations 3(c) are expected to be of similar magnitude as K and L, and they were of course not included in the above calculation.

VI. CONCLUSIONS

A. Exchange parameters

The study of small clusters of Mn^{2+} ions in $CsMn_xMg_{1-x}Br_3$ has enabled us to elucidate the nature of the exchange coupling in this one-dimensional antiferromagnetic system. Magnetic excitations in dimers and trimers proved to be particularly informative. Besides the dominant bilinear exchange term there are significant contributions from biquadratic two-center and three-center terms as well as a bilinear second-nearest-neighbor term. Using these results we are now in a position to interpret the effective J parameter obtained in paper I from the spin-wave dispersion of $CsMnBr_3$. Including the above-mentioned contributions the dispersion of spin waves propagating along the c axis of $CsMnBr_3$ is given by

$$\hbar\omega=10\,|\,-\sqrt{J(J-4J')}-\tfrac{25}{4}(K+2L)\,|\sin\left[\frac{qc}{2}\right], \quad (14)$$

where we have assumed $|J|\gg|J'|,|K|,|L|$. This has to be compared with

$$\hbar\omega=10\,|J_{\text{eff}}|\sin\left[\frac{qc}{2}\right] \quad (15)$$

obtained from the formalism used in paper I, where $|J_{\text{eff}}|$ is the adjustable fit parameter. From a measurement of the spin-wave dispersion we can determine one parameter, $|J_{\text{eff}}|$, but a separation of the various physical contributions to $|J_{\text{eff}}|$ is principally impossible. A numerical comparison of the $|J_{\text{eff}}|$ values obtained from the various measurements is interesting; we have

from spin-wave dispersion measurements:[1]

$$|J_{\text{eff}}|=890\ \mu\text{eV} ,$$

from the study of dimer excitations (with the parameters given in Sec. V A):

$$|J-\tfrac{25}{4}K|=893\ \mu\text{eV} ,$$

from the study of trimer excitations (with the parameters given in Sec. V B):

$$|\,-[J(J-4J')]^{1/2}-\tfrac{25}{4}(K+2L)\,|=884\ \mu\text{eV} .$$

The three values are very similar, indicating that this quantity is a measure of the magnetic energy per Mn^{2+} in the antiferromagnetic state of $CsMnBr_3$. This comparison also explains, at least partly, the difference of 7% between J_{dimer} and J_{trimer}.

B. Cluster versus spin-wave model

In the preceding sections the cluster approach was demonstrated to be very successful and informative in the interpretation of the $CsMn_{0.14}Mg_{0.86}Br_3$ and $CsMn_{0.28}Mg_{0.72}Br_3$ excitation spectra. The limits of this approach become apparent when we go to the more concentrated crystals with $x=0.50$ and 0.75.

It would be desirable to selectively determine the exchange splitting patterns of Mn^{2+} tetramers, pentamers, and higher clusters. But, as shown above, we were only able to measure two tetramer excitations in the $x=0.28$ crystal. There are several limiting factors. The cluster levels become more and more closely spaced as the cluster size increases. The observation of individual transitions is therefore limited by the instrumental resolution. In addition, the total intensity is distributed among an increasingly large number of excitations, so that individual excitations do not have enough weight to be detected. Finally, as x increases, the number of types of clusters contributing to the inelastic scattering increases, amplifying the above problems. It is interesting, though, that the most prominent dimer and trimer excitations at approximately 2, 4, and 6 meV are clearly observable features even in the $x=0.75$ spectra. In the $x=0.50$ spectra they even dominate the inelastic intensity. The predominance of dimer and trimer excitations up to these high concentrations is the result of the 1D nature of our system, by which small clusters are statistically favored compared to a 3D system.

The occurrence of a spin-wave-like excitation with pronounced energy dispersion in the $x=0.75$ and, to a lesser extent, in the $x=0.50$ spectrum clearly demonstrates another limit of the cluster approach. The energies of individual cluster excitations are independent of **Q**. It is, of course, conceivable that for higher clusters a large number of overlapping individual transitions contribute to the total scattering, and the observed energy shift is actually the result of changing relative intensities with **Q**. An interpretation in terms of spin-wave-like excitations is more natural, though, particularly in view of the observed maximum at 8 meV for $\mathbf{Q}=(0,0,1.5)$, which is close to the corresponding value of 8.9 meV for the pure material $CsMnBr_3$.

A spin-wave approach to magnetic excitations in diluted 1D magnetic systems has recently been published.[10] This theoretical approach is clearly inadequate for $x<0.50$ in our system. It is also unable to account for the dispersionless excitations in the $x=0.50$ and $x=0.75$ spectra. However, it appears to be useful for that portion of the inelastic scattering exhibiting the dispersionlike behavior which we observe superimposed on the well-defined dimer and trimer excitations. In view of the average fragment size of Mn^{2+} ions of only three for $x=0.75$, it is understandable that neither a pure cluster nor a pure spin-wave approach can properly account for the observed excitation spectrum. We are presently extending our studies of $CsMn_xMg_{1-x}Br_3$ to larger x values, in order to explore this intermediate region in more detail.

ACKNOWLEDGMENT

Financial support by the Swiss National Science Foundation is gratefully acknowledged.

[1]U. Falk, A. Furrer, H. U. Güdel and J. K. Kjems, preceding paper, Phys. Rev. B **35**, 4888 (1987).
[2]J. Goodyear and D. J. Kennedy, Acta Cryst. **B28**, 1640 (1972).
[3]G. L. McPherson, T. J. Kistenmacher, and G. D. Stucky, J. Chem. Phys. **52**, 815 (1970).
[4]U. Falk, A. Furrer, H. U. Güdel, and J. K. Kjems, Phys. Rev. Lett. **56**, 1956 (1986).
[5]A. Furrer and H. U. Güdel, J. Magn. Magn. Mater. **14**, 256 (1979).
[6]A. Furrer and H. U. Güdel, Phys. Rev. Lett. **39**, 657 (1977).
[7]A. Furrer and H. U. Güdel, J. Appl. Phys. **55**, 1877 (1984).
[8]U. Falk, A. Furrer, J. K. Kjems, and H. U. Güdel, Phys. Rev. Lett. **52**, 1336 (1984).
[9]B. D. Gaulin and M. F. Collins, Phys. Rev. B **33**, 6287 (1986).
[10]A. R. McGurn and M. F. Thorpe, J. Phys. C **16**, 1255 (1983).